Influence of Aerodynamics on Quadrotor Dynamics

MARCO C. DE SIMONE
University of Salerno
Department of Industrial Engineering
Via Giovanni Paolo II, 84084 Fisciano
Italia
mdesimone@unisa.it

SERENA RUSSO
University of Naples, Federico II
Department of Industrial Engineering
Corso Umberto I 40 - 80138 Napoli
Italia
serusso@unisa.it

ALESSANDRO RUGGIERO
University of Salerno
Department of Industrial Engineering
Via Giovanni Paolo II, 84084 Fisciano
Italia
ruggiero@unisa.it

Abstract: The aim of this work is to study the aerodynamics effect of the propellers on the dynamic behaviour of a quadrotor helicopter system. Here an inverse dynamics analysis and a standard PID linear controller for feedback control are considered for a simplified model of UAV represented by a linear under-actuated system. Aerodynamic forces are modeled with the blade element theory to consider the variation of the thrust coefficients with the different flight conditions, in order to calculate the aerodynamic effect of drag and thrust on the rotation of the propellers. This aerodynamic analysis is very useful to predict the dynamic behaviour of the system in presence of wind fields and gives us indications about the type of propellers and motor characteristics to be installed on the UAV. The proposed dynamical model and its control strategies can be source for future works.

Key–Words: UAV, Quadcopter, PID Control, Under-Actuated System.

1 Introduction

A quadrotor UAV is a unmanned mini aerial vehicles (UMAVs) whose lift is generated by four independent rotors. They were initially designed for military application such as surveillance, border patrolling, mine detection, aerial delivery of payload, while, at the moment, they are widely used in several application of life such as civilian purposes like disaster management during floods, earthquakes, fire, commercial missions like aerial photography, television and cinema shootings, and research and development program which need flying vehicles to perform various experiments. They are characterized by vertical take-off and landing (VTOL) capabilities which gives it higher maneuverability and hovering capabilities.

The first real concept of a Quadrotor is due to Breguet and Richet [1]: it was a heavy vehicle capable of flying only over a small height and for short duration. However, over the last years, there has been a great development in the area of quadrotor control, e. g. [2], [3], where the quadrotor dynamics is approximated with a linear system and a standard linear controller is designed (in [4] a PI and PID control has been considered).

The main difficulties in the tracking control of a quadrotor are represented by the parametrization and modelization of external disturbances, such as wind gusts, that could deteriorate the quadrotor abilities of fly and, then, cause instabilities ([5] and [6]). In the flight altitudes typical of these vehicles, quadrotor aerodynamic performances are more sensible to wind fields; so the design of the flight control systems represents one of the most critical aspects to be considered in order to track the desired trajectory in presence of wind external disturbances. One novel aspect that is considered in this article and will be deepened in the successive sperimental activity is represented by the study of the aerodynamics of the propellers that, in general, affects the dynamic response and performance of the UAVs. It depends on the different flight conditions because it is important to include relative wind velocity and gusts (see [6] and [7]). Unless what is already done in several applications, here a different approach will be considered in which the blade element theory will be taken into account in the different flight conditions because there is a change in the trajectory of the drone and also of its velocity, as suggested by the classical propellers theory [8].

In this study, we present a preliminary study for a simplified model of quadrotor in which an inverse dynamic model and a standard PDI linear controller is considered. Inverse dynamics control has been already applied in the past (see [9]) and it represents an approach to nonlinear control design of which the main scope is to construct an inner loop control based on the motion base dynamic model which, in the ideal case, exactly linearizes the nonlinear system and an outer loop control to drive tracking errors to zero [15, 16, 17, 18]. Nonetheless, this technique is based on the assumption of exact cancellation of nonlinear terms, therefore, parametric uncertainty, unmodeled

ISBN: 978-1-61804-316-0

dynamics and external disturbances may deteriorate the controller performance. The standard PID linear controller is considered in the second part of this paper, where the effect of wind fields will be taken into account.

The paper is organized as follows. *Quadrotor Dynamic Model* section discusses the quadrotor dynamic model: it focuses the attention on the set of equations used to model the quadrotor dynamics with particular attention to the treatment of the thrust forces generated by each propeller whose expressions are derived through blade element theory. *Numerical Simulations* contains some details about the prescribed trajectory given to the quadrotor and is divided into two parts: the first part relates with the inverse dynamic analysis of the model, while the second part is dedicated to the feedback control law evaluation in presence of wind disturbances. Final section presents the conclusions.

1.1 Quadrotor dynamic model

In figure 1 the classical configuration of quadrotor is presented. The four rotors are labelled from 1 to 4 and are mounted at the end of each cross arm. One pair of opposite propellers rotates clockwise, while the other pair rotates anticlockwise: in this way it is possible to avoid the yaw drift due to reactive torques and the lateral motion without changing the pitch of the propeller blades. Fixed pitch simplifies rotor mechanics and reduces the gyroscopic effects.

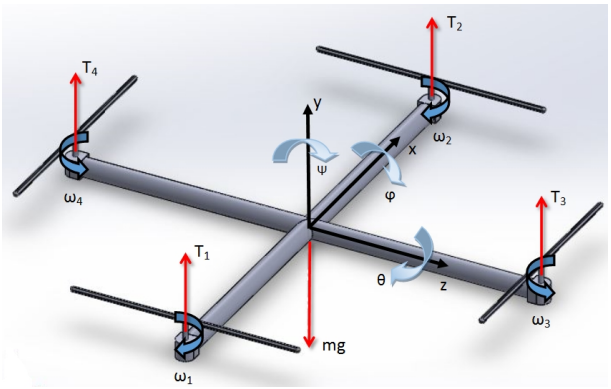

Figure 1: Quadrotor axis system

By imposing different velocities to different propellers, so differential aerodynamic forces and moments, it is possible to control the UAV. For hovering, all four propellers need to rotate at same speed. The vertical motion is allowed because the speed of all four propellers is increased or decreased by the same amount, simultaneously. In order to pitch and move laterally in the x direction, speed of propellers 1 and 2 is changed conversely. Similarly, for roll and corresponding lateral motion in the z, speed of propellers 3 and 4 is changed conversely. Yaw along the y axis is possible when the speed of one pair of two oppositely placed propellers is increased while the speed of the other pair is decreased by the same amount. This way, overall thrust produced is same, but differential drag moment creates yawing motion. In spite of four actuators, the quadrotor is still an under-actuated system.
In the hypothesis that the center of mass coincides with the origin of body frame B, the propellers are rigid in plane and the structure is rigid and symmetrical, the translational dynamics of the drone in the coordinate system I can be written as

$$\mathbf{M}\dot{\mathbf{v}} = -\begin{bmatrix} 0 \\ mg \\ 0 \end{bmatrix} + \mathbf{R}_{\{I-B\}}\begin{bmatrix} 0 \\ T \\ 0 \end{bmatrix} - \mathbf{F}_D + \mathbf{F}_W \quad (1)$$

where I is the inertial frame, $\mathbf{v}$ is the velocity vector of the center of gravity of the aerial vehicle in the inertial frame, $\mathbf{M}$ represents the mass matrix, $\mathbf{R}_{\{I-B\}}$ is the rotation matrix from the body to the inertial frame, g is the gravitational acceleration, m is the total mass of the system, $T = \sum T_i$ is the total upward thrust, $\mathbf{F}_D = [F_{Dx}, F_{Dy}, F_{Dz}]^T$ is drag force acting opposite to the relative motion of the quadrotor object moving with respect to the surrounding air and $\mathbf{F}_W = [F_{Wx}, F_{Wy}, F_{Wz}]^T$ represents the wind disturbance.
gives the rotational acceleration of the body frame is given by Euler's equation of motion

$$\mathbf{I}\dot{\omega} = -\omega \times \omega\mathbf{I} + \Gamma \quad (2)$$

where $\mathbf{I}$ is the 3×3 inertia matrix of the system, ω is the angular velocity vector and $\Gamma = [\tau_x, \tau_y, \tau_z]^T$ is the torque applied to the frame. As already said, differences in rotor thrust produce rotation along the axis. Rolling is caused by the torque along the x-axis, $\tau_x = d(T_4 - T_3)$ where d is the distance of the propeller from the center of gravity of the system. Pitching torque, $\tau_z = d(T_2 - T_1)$, is responsible of the rotation of the frame along the z-axis. Yawing rotation, instead, is due to the total reaction torque of each propeller which acts at rotating the airframe in the opposite direction of its rotation $\tau_y = Q_1 + Q_2 - Q_3 - Q_4$.
In this work, a simplified $2D$ model is considered where the rolling, yawing, traslation along the z axis balance equations are satisfied, so that the set of equations simplify to

$$\begin{cases} -m\ddot{x} + T_x - F_{Dx} + F_{Wx} = 0 \\ -m\ddot{y} - mg + T_y - F_{Dy} + F_{Wy} = 0 \end{cases} \quad (3)$$

The pitch angle cannot be arbitrarily set, but it is obtained from the following condition constraint

$$\frac{T_x}{T_y} = tan(\theta) \simeq \theta, \quad (4)$$

The moment balance equation (2) becomes a scalar equation because the only pitching torque τ_z is different from zero.

2 Aerodynamic forces and torques

The resulting thrust force T_i produced from each propeller is proportional to the square of its angular speed rotation using momentum theory [8] according to the following relation

$$T_i = b\omega_i^2, i = 1, 2, 3, 4; \tag{5}$$

where parameter b needs to be determined for each propeller. Since the quadrotor is characterized by a time constant of the motor dynamics less than $1ms$ that is faster than the time scale typical of rigid body dynamics, it is possible to assume that T_i changes istantaneously. The main error of this model is represented by the simplistic assumption underlying formula 5 that the thrust forces are directly proportional to the square of the motor speed. In reality they are complex functions of the motor speed and environmental conditions.
The drag force is imposed to have the following relation (see [11]), so it is proportional to the translational velocity of drone

$$\mathbf{F}_D = \frac{1}{2}\rho S C_D \mathbf{V}^2, \tag{6}$$

where S is the cross-sectional area of the quadrotor, $C_D = diag(C_{Dx}, C_{Dy}, C_{Dz})$ is the traslational drag coefficient.

2.1 Aerodynamics of vertical and forward flight

A rotor generates thrust by inducing a velocity on the air that passes through it. In hovering (that is the situation in which the quadrotor maintains a constant position over the ground), the thrust ($T_{i,h}$) generated from each propeller is linked to the (vertical) induced velocity (v_h), that is the velocity induced on the air without relative velocity between the rotor and the air. It is derived from the momentum analysis as

$$v_h = \sqrt{\frac{T_{i,h}}{2\rho A}}. \tag{7}$$

The relative velocity between the rotor plane and the surrounding air (V) and the pitch angle, also, influence the thrust produced by each rotor (see figure 2).

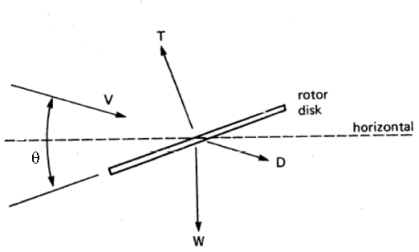

Figure 2: Diagram of rotor.

According to the blade element theory, it is possible to find an expression for the thrust like this

$$T_i = c_t \rho \pi R_p^4 \omega_i^2. \tag{8}$$

Here ρ is the air density and R_p represents the radius of the propeller. When $\theta = \pi/2$, the quadrotor is in vertical (climb or descendent) flight and the thrust coefficients (c_t) can be derived with the following expression [14]

$$c_t = \frac{nca}{4\pi R_p}\Big(\beta_t - \frac{v_h \pm V}{\omega R_p}\Big), \tag{9}$$

where β_t is the pitch angle at the blade tip that is function of rotor geometry alone as we are considering fixed pitch rotors [14], a is the lift slope curve, n is the number of blades on each propeller and c is the blade chord. Formula 9 is derived in the hypothesis of constant chord and linear twist and assuming uniform inflow. Given the vertical velocity $\dot{y}$ and the geometric parameters, it is possible to find the ω_i which produces a given thrust at the current vertical velocity.
In forward flight, it is important to consider the angle of attack (θ) to the model, so the equation for the thrust coefficient becomes

$$c_t = \frac{nca}{2\pi R_p}\Big(\frac{\beta_t}{3} + \frac{V^2 \beta cos^2\theta}{2\omega_i^2 R_p^2} + \frac{V sin\theta + v_h}{2\omega R_p}\Big). \tag{10}$$

In order to test the reliability of the above expression of c_t (formula 9), the results are compared with an experimental database ([19]). Figure 3 depicts the comparison between the values of the thrust coefficients obtained from the database (the blue circles) and the curve obtained from formula 9: the thrust coefficients are plotted against J

$$J = \frac{V}{N D_p}, \tag{11}$$

where *N* is the angular velocity in *rpm* and D_p represents the diameter of the propeller.
Fig. 4 displays the thrust coefficient trends for the interesting range of *N* of our quadrotor. One of the novel

ISBN: 978-1-61804-316-0

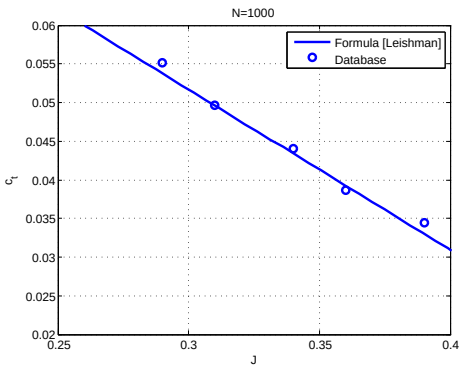

Figure 3: Thrust coefficients.

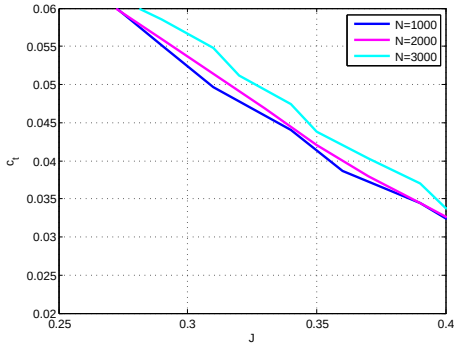

Figure 4: Thrust coefficients.

contribution of this paper is the introduction of a variation of the c_t coefficients for every flight conditions, instead of using a constant value of it and then of b as it is generally done in these applications. These coefficients cannot be directly derived from Fig. 4 because J is function of N that is the parametrization constant of the curve, for this reason the corrected values have been extrapolated by trial.

3 Numerical Simulations

The dynamic model, that includes rotor dynamics and external perturbation like drag force and wind disturbances, is developed using a multibody approach consisting in interconnected rigid components by different kinds of joints. Mass and inertia matrices are obtained by using a CAD model of the quadcopter and are represented by the following expressions (12 and 13), i.e.

$$\mathbf{M} = \begin{bmatrix} 0.37958 & 0 & 0 \\ 0 & 0.37958 & 0 \\ 0 & 0 & 0.37958 \end{bmatrix} kg \qquad (12)$$

Segment	$x_{in}[m]$	$x_{fin}[m]$	$y_{in}[m]$	$y_{fin}[m]$	$t^i_{fin}[s]$	$T_{fin}[s]$
1	0	0	0	5	10	10
2	0	100	5	5	40	50
3	100	100	5	0	10	60

Table 1: Waypoint Coordinates used for desired trajectory

$$\mathbf{J} = \begin{bmatrix} 0.0053 & -2.492e-05 & 1.249e-05 \\ -2.492e-06 & 0.0092 & 7.245e-05 \\ 1.249e-05 & 7.245e-05 & 0.0043 \end{bmatrix} kgm/s^2. \qquad (13)$$

The mathematical model used for the evaluation of feedforward control is reported in eq. 14, where $\mathbf{T} = \sum_{i=1}^{4} \mathbf{T}_i$ and $\tau_z = d(T_2 - T_1)$, i.e.

$$\begin{cases} \mathbf{T} = \mathbf{M}\dot{v} + \mathbf{F}(\dot{v}) \\ \tau_z = I_{zz}\ddot{\theta} + M_D(\dot{\theta}). \end{cases} \qquad (14)$$

In the general case, $\mathbf{F}$ contains the gravity effects, the aerodynamic drag terms and the wind disturbances contributions, while M_D is function of the aerodynamic drag moment.

For the given trajectory, reported in figure 5(a), the law of motion for the two degrees of freedom system is evaluated by using a quintic polynomial function. Smoothness represents an important characteristic of the law of motion, so that position and orientation vary slowly and their temporal derivatives are continuous with time. The respective boundary conditions for every segment of the trajectory are reported in tabular 1, while velocity and acceleration boundary conditions are all set equal to zero. By solving system 14, it is possible to derive the laws of motion for the three degrees of freedom (x-axis, y-axis and pitch angle θ) and the feedforward control laws of the four propeller T_1, T_2, T_3 and T_4 necessary to obtain the desired trajectory.

From the thrust forces, one can evaluate the angular velocity that each motor must deliver in order to ensure the tracing of the desired trajectory by using eq. 5. Here we have verified if it is valid the hypothesis, that is generally made in such applications [3] [11], of a constant parameter b and so of a constant thrust coefficient c_t. For this reason, we have extrapolated c_t, that it is function not only of N, but also of the relative velocity v, from fig.4 for each integration time and we have verified that the results obtained here are different from the case in which a constant value is considered. In this way it is possible to have the corrected angular velocities for every time step.

ISBN: 978-1-61804-316-0

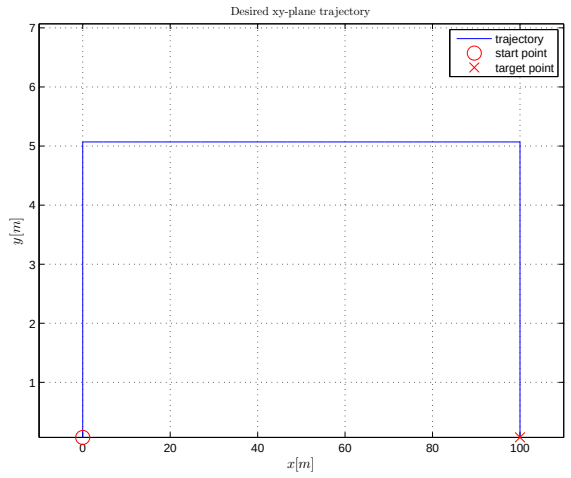

(a)

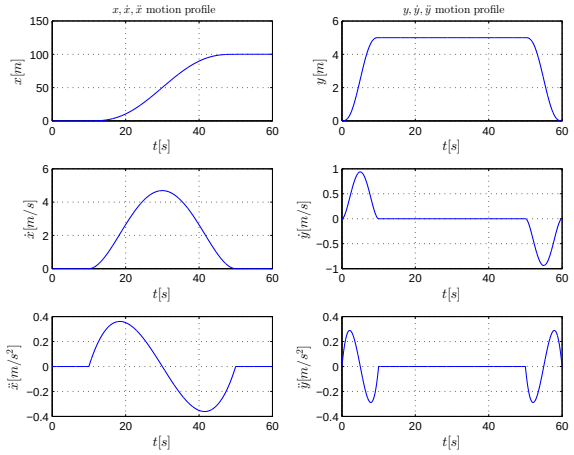

(b)

Figure 5: (a) Target Trajectory, (b) Law of Motion for x-axis and y-axis

.

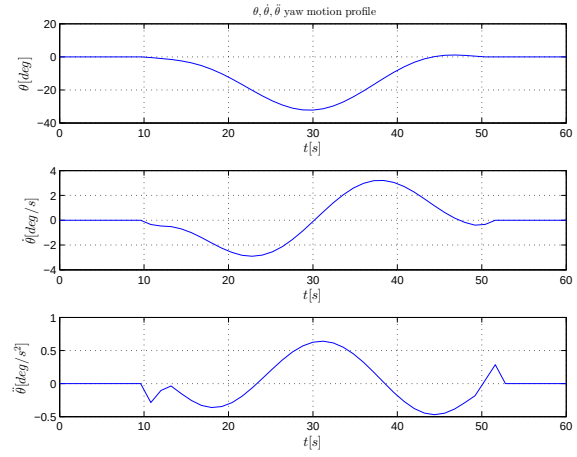

Figure 6: Derived Law of Motion for Pitch Angle

3.1 Inverse Dynamics Analysis in absence of wind disturbances

In this section, the effect of wind disturbances is not considered in 14, so $\mathbf{F}$ only contains the gravity term and aerodynamic drag contributions, i.e.

$$\mathbf{F}(\dot{v}) = \mathbf{F}_D(\dot{v}) - m\mathbf{g}. \tag{15}$$

By solving system 14 with the above expression for $\mathbf{F}$, it is possible to derive the laws of motion for the two degrees of freedom, x-axis, y-axis and the bounded pitch angle θ, that are depicted in figures 5(a), 5(b) and 6). Figures 5(a), 5(b) and 6 demonstrate that they are in agreement with the given trajectory and laws of motion. The thrust laws are reported in fig. 7, in which the curves that refer to propellers 4 and 3, can be overlapped because of the simplified $2D$ configuration. The angular velocities of each propeller

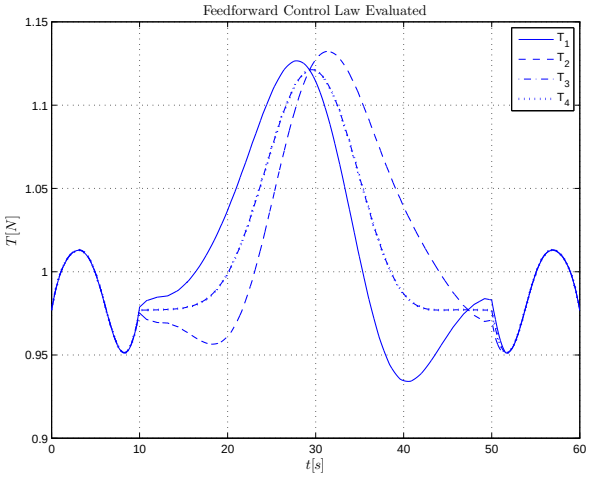

Figure 7: Thrust Forces Evaluated by Inverse Dynamics Analysis

are calculated from the thrust forces and the interpolated thrust coefficients (using eq. 5 and fig. 4) and are plotted in fig. 8: the different sign is due to the different direction of rotation of each propeller, necessary to lateral displacement and the balance of moments. In these cases, thrust coefficients are variable for each time step: by comparing these results with those obtained in a first approximation in which a constant value of b has been considered, we have observed differences of the order of $100rpm$ in the calculated angular velocities.

Forward Dynamics Analysis in presence of wind disturbances

In this section, a feedback control has been considered in order to take into account the aerodynamic distur-

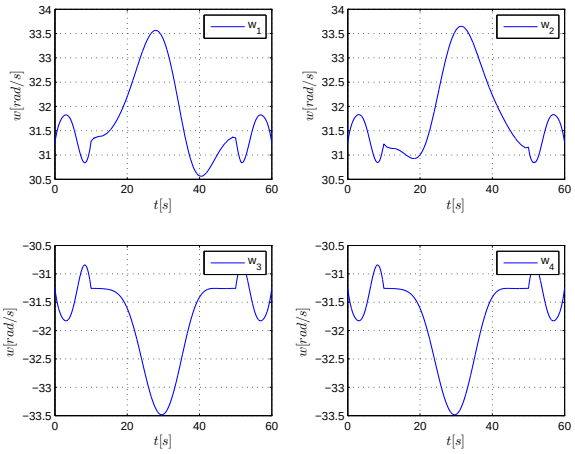

Figure 8: Angular Velocity of each Propeller

bances represented by wind gusts. To counteract these effects a PID controller is developed, i.e.

$$\mathbf{F}_{fb}(t) = \mathbf{k}_p \mathbf{e}(t) + \mathbf{k}_d \dot{\mathbf{e}}(t) + \mathbf{k}_i \int_0^t \mathbf{e}(t)dt, \qquad (16)$$

where $\mathbf{k}_p$, $\mathbf{k}_d$ and $\mathbf{k}_i$ respectively represent the proportional, derivative and integral gain values vector. The error signal vector has the following expression

$$\mathbf{e}(t) = \begin{bmatrix} e_x(t) \\ e_y(t) \end{bmatrix} = \begin{bmatrix} x_{ref} - x(t) \\ y_{ref} - y(t) \end{bmatrix}, \qquad (17)$$

where $[x_{ref}, y_{ref}]^T$ is the desired solution. As suggested by Chen *et al.* ([11]), the wind field is modeled as an external force term, so that, in the balance equations 14, $\mathbf{F}$ is the sum of three contributions, i.e.

$$\mathbf{F}(\dot{v}) = \mathbf{F}_D(\dot{v}) - m\mathbf{g} + \mathbf{F}_W(v). \qquad (18)$$

To test the robustness of the controller, the vehicle is subjected to two wind fields $\mathbf{W}_1 = [2, 0]^T$ m/s and $\mathbf{W}_2 = [2, 1]^T$ m/s.

Figures 9(a) and 9(b) depict the comparison between the open–loop real trajectories covered by the UAV under feed–forward control law in presence of wind gusts (continuous line) and the desired trajectory (dashed line): in both cases of wind velocities, it is possible to observe a discrepancy between the two trajectories.

Figures 10(a) and 10(b) display the effect of the closed–loop control in the comparison between the real trajectory (continuous line) and the desired one (dashed line). Unlike the previous case, curves perfectly overlap: this evidence demonstrates the effectiveness of the projected closed–loop control.

Finally the two control laws have been traced back,

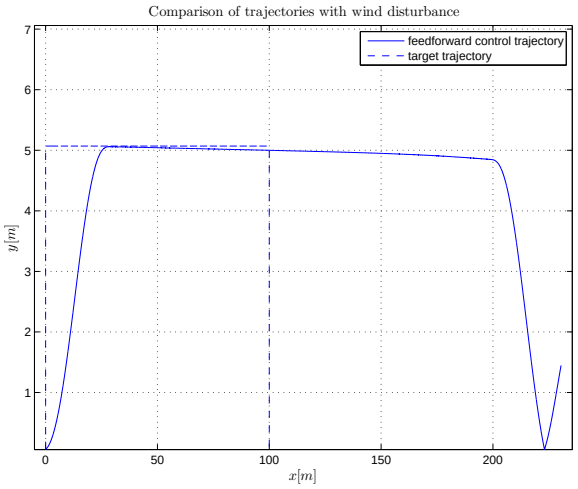

(a)

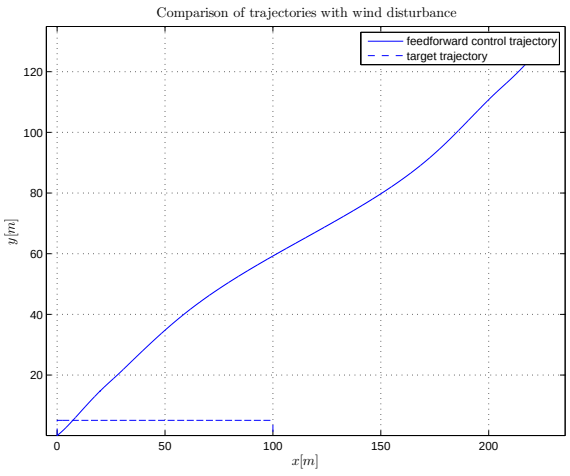

(b)

Figure 9: Comparison between the Open Loop Trajectories Subjected to Wind Fields and the Desired Trajectories: (a) refers to $\mathbf{W}_1$, (b) refers to $\mathbf{W}_2$

.

ISBN: 978-1-61804-316-0

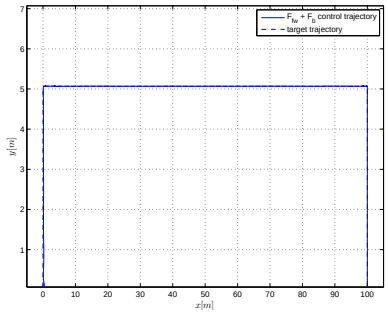

(a)

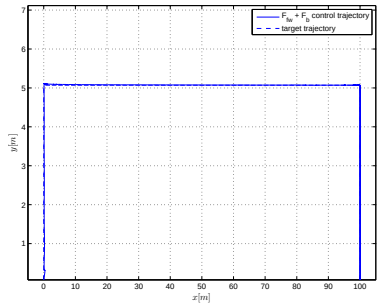

(b)

Figure 10: Comparison between the Closed Loop Trajectories Subjected to Wind Fields and the Desired Trajectories: (a) refers to $\mathbf{W}_1$, (b) refers to $\mathbf{W}_2$.

through the use of eq 5, to the values of the angular velocities required by the four engines and have been reported in figure 11. The first oscillations that characterize each curve of the angular velocity relative to $\mathbf{W}_1$ for the first time step are due to the sudden arrangement that the system must have in order to adapt to the presence of the wind field.

4 Conclusion

In this paper a $2D$ dynamical model of an underactuated UAV has been presented. Firstly, an inverse dynamics analysis has been performed on the model for feed-forward thrust evaluation from a given trajectory. In this phase only aerodynamics effects of drag have been considered and pitch angle motion law has been evaluated together with the pitching torque required.

Thereafter, a linear PID controller has been designed for feedback control in presence of wind fields. The comparison between the real and the desired paths have demonstrated the effectiveness of the projected closed–loop control.

For both cases of open–loop and closed–loop thrust laws, we have verified the reliability of the hypothesis of constant thrust coefficient that is generally made in

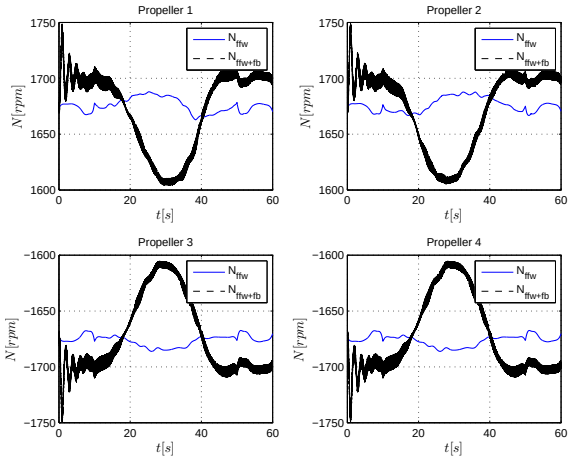

(a)

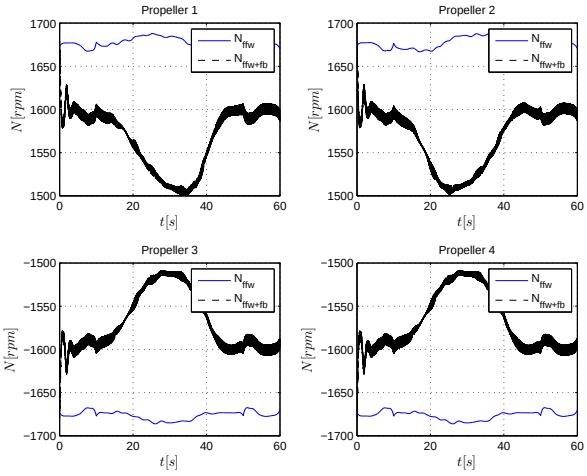

(b)

Figure 11: Comparison between the Open Loop (continuous line) and the Closed Loop (dashed line) Trajectories Subjected to Wind Fields in term of the angular velocity of each propeller: (a) refers to $\mathbf{W}_1$, (b) refers to $\mathbf{W}_2$.

ISBN: 978-1-61804-316-0

these applications. Since it is generally function of the engine rpm, of the thrust forces required and of relative velocity of the vehicle and its variation with these parameters is not neglibible, all the values are extrapolated from different curves parameterized as a function of the rpm for every time steps. By comparing these results with those obtained by using a constant coefficient, there is an error in estimating the correct rpm of about ± 100.
The considerations developed in this work about a simplified $2D$ will be the starting point for a subsequent analysis of a $3D$ model in which a variation of the thrust coefficient will be taken into account.

References:

[1] J. G. Leishman. *The Breguet–Richet Quad Rotor Helicopter of* 1907. $http : //www.glue.umd.edu/ leishman/Aero$ (EURODYN 2011), accessed Jan. 2009.

[2] M. Belkheiri, A. Rabhi, A. E. Hajjaji, C. Pegard. *Different linearization control techniques for a quadrotor system*. 2nd. Int. Conf. on Communications, Computing and Control Applications (CCCA), 1–6, 2012.

[3] B. Zhu and W. Huo, *Trajectory linearization control for a quadrotor helicopter.* In 8th IEEE Int. Conf. on Control and Automation (ICCA), pp. 34-39, June 2010.

[4] S. L. W. Gabriel, M. Hoffmann and C. J. Tomlin, *Quadrotor helicopter trajectory tracking control.* In Proc. of the AIAA Guidance Navigation and Control Conference, 2008.

[5] K. Alexis, G. Nikolakopoulos and A. Tzes, *Switching model predictive attitude control for a quadrotor helicopter subject to atmospheric disturbances*, Control Engineering Practice, vol. 19, pp. 1195-1207, 2011.

[6] C. Powers, D. Mellinger, A. Kushleyev, B. Kothmann and V. Kumar, *Influence of Aerodynamics and proximity effects in quadrotor flight*, Proceedings of the 13th International Symposium on Experimental Robotics, Quebec city, Canada, June 17-21, 2012.

[7] H. Huang, G.M. Hoffmann, S.L. Waslander and C.J. Tomlin, *Aerodynamics and control of autonomous quadrotor helicopters in aggressive maneuvering*, Proceedings of the IEEE International Conference on Robotics and Automation (ICRA '09), pp. 32773282, 2009.

[8] A. R. S. Bramwell, G. Done and D. Balmford *Bramwells Helicopter Dynamics,* 2^{nd} *ed.*, Butterworth Heinemann, Oxford, UK, 2001.

[9] M. Becerra-Vargas and E. Morgado Belo, *Inverse Dynamics control for a 3DOF quadrotor*, ABCM Symposium Series in Mechatronics, Vol.5, 2012.

[10] F. Nilvetti and M. C. De Simone, *Test-Rig for Identification and Control Applications*, Proceedings of International Conference on Vibration Problems (ICOVP-2013), Lisbon, Portugal, 2013.

[11] Y. Chen, Y. He and M. Zhou, *Modeling and control of a quadrotor helicopter system under impact of wind field*, Research Journal of Applied Sciences, Engineering and Technology, 6(17), pp. 3214-3221, 2013.

[12] P. Corke, *Robotics, Vision and Control*, Springer Tracts in Advanced Robotics, 2nd ed., 2013.

[13] L. Derafa, T. Madani and A. Benallegue, *Dynamic Modelling and Experimental Identification of Four Rotors Helicopter Parameters*, Industrial Technology, 2006. ICIT 2006. IEEE International Conference on, IEEE, pp. 1834–1839, 2006.

[14] J.G. Leishman, *Principles of Helicopter Aerodynamics*, Cambirdge Aerospace Series, 2000.

[15] M.C. De Simone, A. Ruggiero, Z. Chavez, D. Guida *Instability in Disk Brake Systems*, International Conference of Theoretical and Applied Mechanics 2015, Salerno, 2015.

[16] M.C. De Simone, A. Ruggiero, Z. Chavez, D. Guida *Dry Friction Influence on the Response of a Mechanical System with Two DOFs*, International Conference of Theoretical and Applied Mechanics 2015, Salerno, 2015.

[17] A. Ruggiero, M.C. De Simone, D. Russo, D. Guida *Spectral Properties of Orchestral Instruments Measured in the Concert Hall of a Public School*, International Conference of Theoretical and Applied Mechanics 2015, Salerno, 2015.

[18] M. C. De Simone, D. Guida *Dry Friction Influence on Structure Dynamics*, International Conference on Computational Methods in Structural Dynamics and Earthquake Engineering 2015, Crete Island, 2015.

[19] http://www.drivecalc.de/